

## Evaluation of Electron Temperature Dependence of Current Decay Time in the Large Helical Device

Y. Shibata<sup>1</sup>, N. Ohno<sup>1</sup>, M. Okamoto<sup>2</sup>, K.Y. Watanabe<sup>3</sup>, M. Goto<sup>3</sup>

<sup>1</sup> Dept. of Energy Eng. and Sci., Graduate School of Eng., Nagoya Univ., 464-8603, Nagoya, Japan

<sup>2</sup> Ishikawa National College of Technology, 929-0392, Ishikawa, Japan

<sup>3</sup>National Institute for Fusion Science, 509-5292, Toki, Japan

### 1. Introduction

The precise prediction of current decay time during tokamak disruptions is one of the most critical issues in next generation tokamaks such as ITER because the current decay time  $t_d$  determines electromagnetic forces acting on in-vessel components. The database of current decay times during disruptions has also been set up among the different tokamaks based on so called L/R model [1]. In this model,  $t_d$  normalized by the plasma cross-section area  $S$  is proportional to  $T_e^{3/2}$ , where  $T_e$  is electron temperature. Some problems, however, have been found that data of the normalized  $t_d$ 's have large scatters among different tokamaks, as well as different shots. The validity of the L/R model has not been confirmed yet, moreover the understanding of the determination mechanism of  $t_d$  is rather poor at this moment. The difficulty may come from the co-existence of different mechanisms to determine  $t_d$  during the current decay, such as atomic/molecular processes associated with electron cooling and rapid change of magnetic surface in tokamaks. On the other hand, in helical devices, we can distinguish the influences of atomic/molecular processes and the magnetic surface change on the current decay because the helical devices always keep magnetic surfaces externally. Therefore, the systematic study of the current decay in the helical system can give better understanding of the mechanism of the current decay in tokamaks.

On the other hand, in helical devices, it is anticipated that the bootstrap current and Ohkawa current are generated. It is necessary to control the spontaneous current because the magnetic field reduced by the spontaneous current disturbs the equilibrium of magnetic field. It is also one of the important issues to study the physics of plasma current decay in helical systems in order to control the

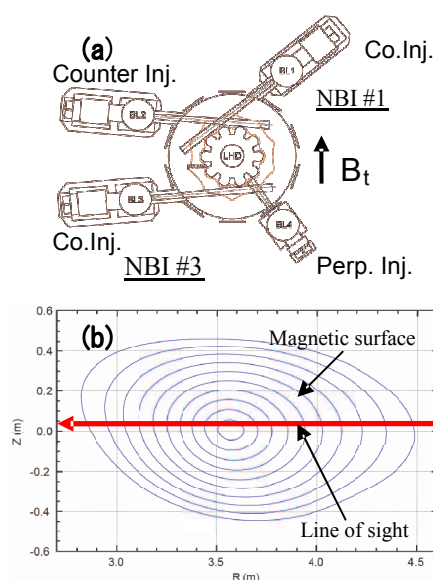


Fig. 1 (a) Schematic view of Neutral Beam Injection system in LHD, (b) Map of the magnetic surfaces at a magnetic axis of  $R_{ax}=3.6m$  and  $B_{ax}=2.75T$ . The  $Z$  and  $R$  axes indicate the vertical and major radius, respectively. The red line is the line of sight for spectroscopy.

magnetic confinement. Then, we carried out the current decay experiment in the Large Helical Device (LHD) to understand the mechanism for the current decay time.

### 2. Experimental setup

Figure 1 (a) shows schematic view of neutral beam injection (NBI) system in the LHD. In order to generate plasma current, we used NBI #1 and NBI #3. The current decay was observed by turning off the NBIs. In order to evaluate L/R model, we measured the time evolution of  $T_e$  during the current decay by using two methods, i.e., from the measurement of the emission intensities of HeI lines with a high time resolution spectrometer (maximum: 16 $\mu$ s) and from Thomson scattering measurement with a time resolution of 33ms. Figure 1 (b) shows the line of sight of the spectroscopy. It is possible to evaluate the electron temperature and density from HeI intensity line ratios by comparing them to the CR model calculation [2], the electron temperature is obtained from the intensity ratio of 667.8nm ( $2^1P-3^1D$ )/728.1nm ( $2^1P-3^1S$ ) and the electron density is from the intensity ratio of 728.1nm ( $2^1P-3^1S$ )/ 706.5nm ( $2^3P-3^3S$ ).

### 3. Experimental result

Figure 2 (a) and (b) show the waveforms of plasma current and NB Injection power during the current decay. After turning off the NBI at  $t = 3.3$ s, the plasma current began to decrease. The time evolution of the plasma current shows slow decay phase ( $t = 3.3$ s ~) and fast decay phase ( $t = 3.95$ s~) as shown in (a).

#### 3.1 Slow decay phase

Figure 3 shows  $T_e$  profiles in the slow decay phase ( $t = 3.3 - 3.95$ s). In order to estimate the current decay time by using L/R model in the slow decay phase, we evaluated the plasma

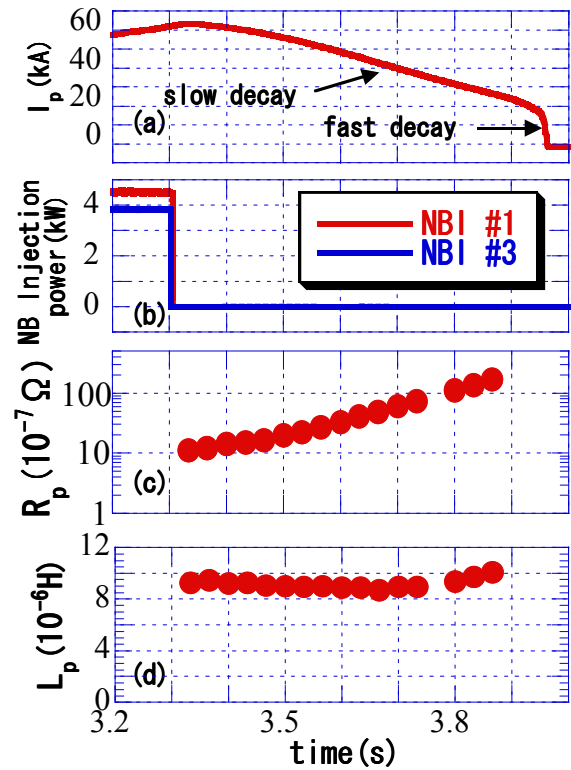


Fig. 2 Temporal evolution of (a) plasma current  $I_p$ , (b) NB Injection power, (c) plasma resistance  $R_p$ , (d) plasma inductance  $L_p$  in slow decay phase.

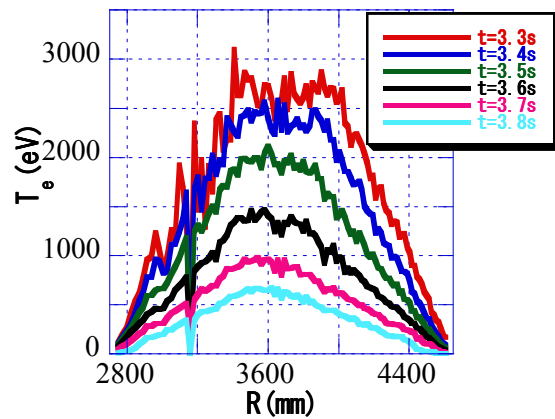


Fig. 3 Temporal evolution of electron distribution measured by Thomson scattering system in slow decay phase.

resistance  $R_p$  and the plasma inductance  $L_p$  from  $T_e$  profiles. First, we calculated the plasma resistance by considering the neo-classical effect from  $T_e$  profile by using Eq. (1) and (2).

$$R_p = R_0 / \int_0^a r \sigma F(r/a) dr \quad \dots(1)$$

$$\sigma = 1/\eta = 1/(1.65 \times 10^{-9} \times Z_{\text{eff}} \times \ln \Lambda \times T_e^{-3/2}) \quad \dots(2)$$

where  $R_0$  is major radius and  $a$  is minor radius,  $Z_{\text{eff}}$  is effective charge, and  $\ln \Lambda$  is Coulomb logarithm. We consider the neo-classical effect on  $R_p$ .  $F(r/a)$  in Eq. (1) represents the ratio of the plasma resistivity  $\eta_{\text{neo}}$  by considering the neo-classical effect as shown in Fig 4 to the spitzer plasma resistivity  $\eta_{\text{spitzer}}$ . We assumed the effective charge  $Z_{\text{eff}}=3$ . Second, we evaluated the time evolution of plasma inductance  $L_p$  by using Eq.(3)-(5).

$$B_\phi(r) = \mu_0 \int_0^r j dS / 2\pi R_0 \quad \dots(3)$$

$$L_p = \mu_0 R_0 \left( \frac{1}{2} I_i + \ln \frac{8R_0}{a} - 2 \right) \quad \dots(5)$$

where  $B_\phi$  is poloidal magnetic field and  $B_{\phi a}$  is poloidal magnetic field at  $r = a$ . When we evaluated  $B_\phi(r)$ , it is assumed that the current density  $j$  is proportioned to  $T_e^{3/2}$ . Figure 2 (c) and (d) show the time evolution of  $R_p$  and  $L_p$  calculated from  $T_e$  profiles. As shown in Fig. 2, it is found that  $R_p$  changes drastically in the slow decay phase whereas  $L_p$  is almost constant. Because NBI components would survive even after turning the NBI off, we need to consider the slowing down of high energy particles associated with NBI. Eq. (6) shows the circuit equation of  $I_p$  by taking the slowing down of the energetic particles into account, where  $t_{\text{slow}}$  is given by Eq. (7) .

$$L \frac{dI_p}{dt} + RI_p = RI_{N10} \exp\left(-\frac{t}{\tau_{\text{slow}}}\right) \quad \dots(6)$$

Figure 5 shows comparison between  $t_{\text{cal}}$  and  $t_{\text{exp}}$ .  $t_{\text{exp}}$  is the plasma current decay time obtained from the plasma current waveform. It is found that  $t_{\text{exp}}$  and  $t_{\text{cal}}$  has correlation.

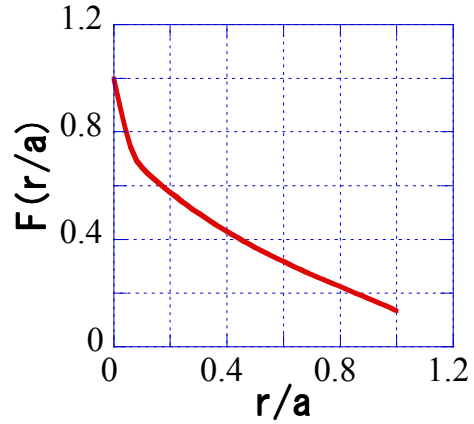


Fig. 4 The relationship between  $r/a$  and  $F(r/a)$ .  $F(r/a)$  is the ratio of  $\eta_{\text{neo}}$  and  $\eta_{\text{spitzer}}$ .  $\eta_{\text{spitzer}}$  is the spitzer resistivity and  $\eta_{\text{neo}}$  is the resistivity by considering the neo-classical effect.

$$I_i = 2 \int_0^a B_\phi^2 r dr / a^2 B_{\phi a}^2 \quad \dots(4)$$

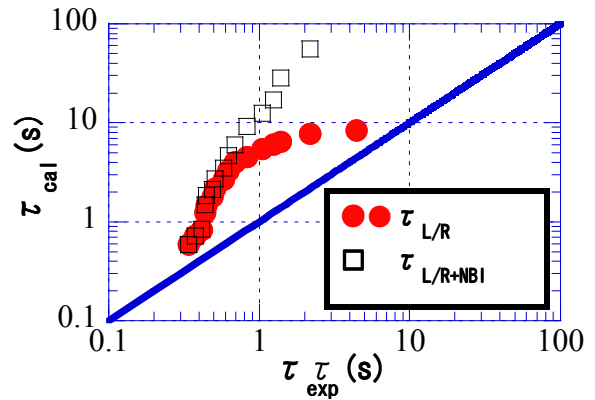


Fig. 5 The evaluation of plasma current decay time.  $\tau_{L/R}$  is the plasma current decay time calculated by L/R model and  $\tau_{L/R+NBI}$  is the plasma current decay time calculated by Eq. (6).  $\tau_{\text{exp}}$  is the plasma current decay time calculated by the experimental plasma current waveform. The solid line has shows  $\tau_{\text{cal}} = \tau_{\text{exp}}$ .

$$\tau_{\text{slow}} = 2 \times 10^{-1} \frac{A T_e^{3/2}}{Z_i^2 (n_e / 10^{20}) \ln \Lambda} \quad \dots(7)$$

However both  $t_{L/R}$  and  $t_{L/R+NBI}$  are larger than  $t_{exp}$ .

### 3.2 Fast decay phase

Figure 6 (c) shows the time evolution of HeI emission intensities (667nm, 706nm, 728nm). The HeI emission intensities increase dramatically at  $t \sim 2.4s$ , which indicates that the volume plasma recombination occurs. In order to evaluate  $T_e$  before  $t = 2.4s$ , we used HeI intensity ratio. Boltzman plot method is used in order to determine  $T_e$  when the volume plasma recombination occurs around  $t = 2.4s$  [3]. In the fast decay phase, HeI emission intensities begin to decrease. It seems that the whole plasma becomes the recombining regime and the plasma volume could decrease. It is found that the fast current decay in LHD was related to the atomic/molecular processes. Unfortunately, L/R model was not able to be evaluated in the fast decay phase because the plasma inductance  $L_p$  could not be obtained.

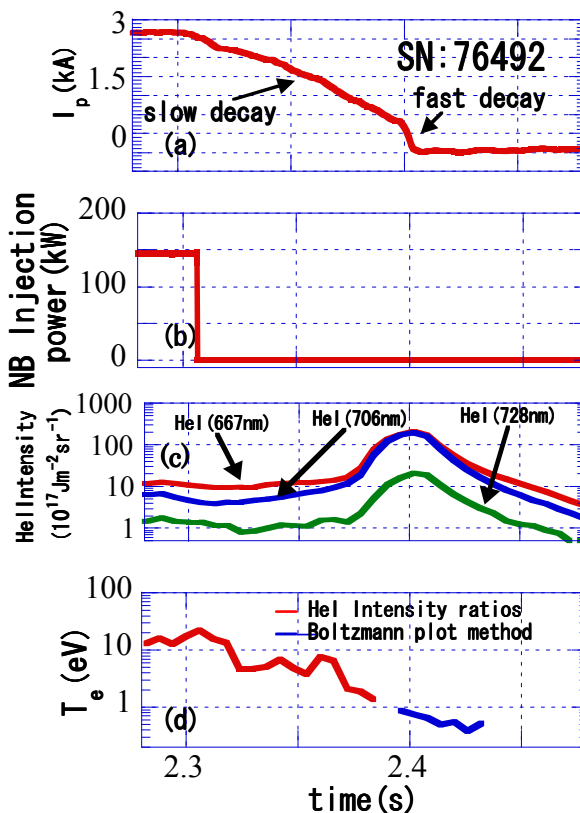


Fig.6 The time evaluation of (a)plasma current  $I_p$ , (b)NB Injection power, (c)HeI emission intensities(667nm,706nm,728nm), (d)electron temperature obtained by the spectroscopic method.

### 4. Conclusion

We carried out the experiment on current decay by using NBI system in the LHD. We found that there are two phases during the plasma current decay, the slow decay phase and the fast decay phase. In the slow decay phase, we evaluated the plasma resistance and inductance from  $T_e$  profiles. We evaluated the current decay time from the L/R model, and it is found that the current decay time was related to the electron temperature. In the fast decay phase, we found from spectroscopic observation that the rapid plasma current decay in LHD was related to the atomic/molecular processes. In future works, we need to evaluate directly the plasma inductance and effective charge in the current decay phase.

### Reference

- [1]ITER Physics Basis, Nuclear Fusion 47(2007)
- [2]M. Goto, J. Quant. Spectr. Radiat. Trans. 76(2003) 331
- [3]D. Nishijima et al., J. Nucl. Mater. 290-293(2001) 688